Proudman
Oceanographic
Laboratory

Measurements of Turbulence and Acoustic Detection of Bedload in a Mountain River

JJ Williams

Report No. 36

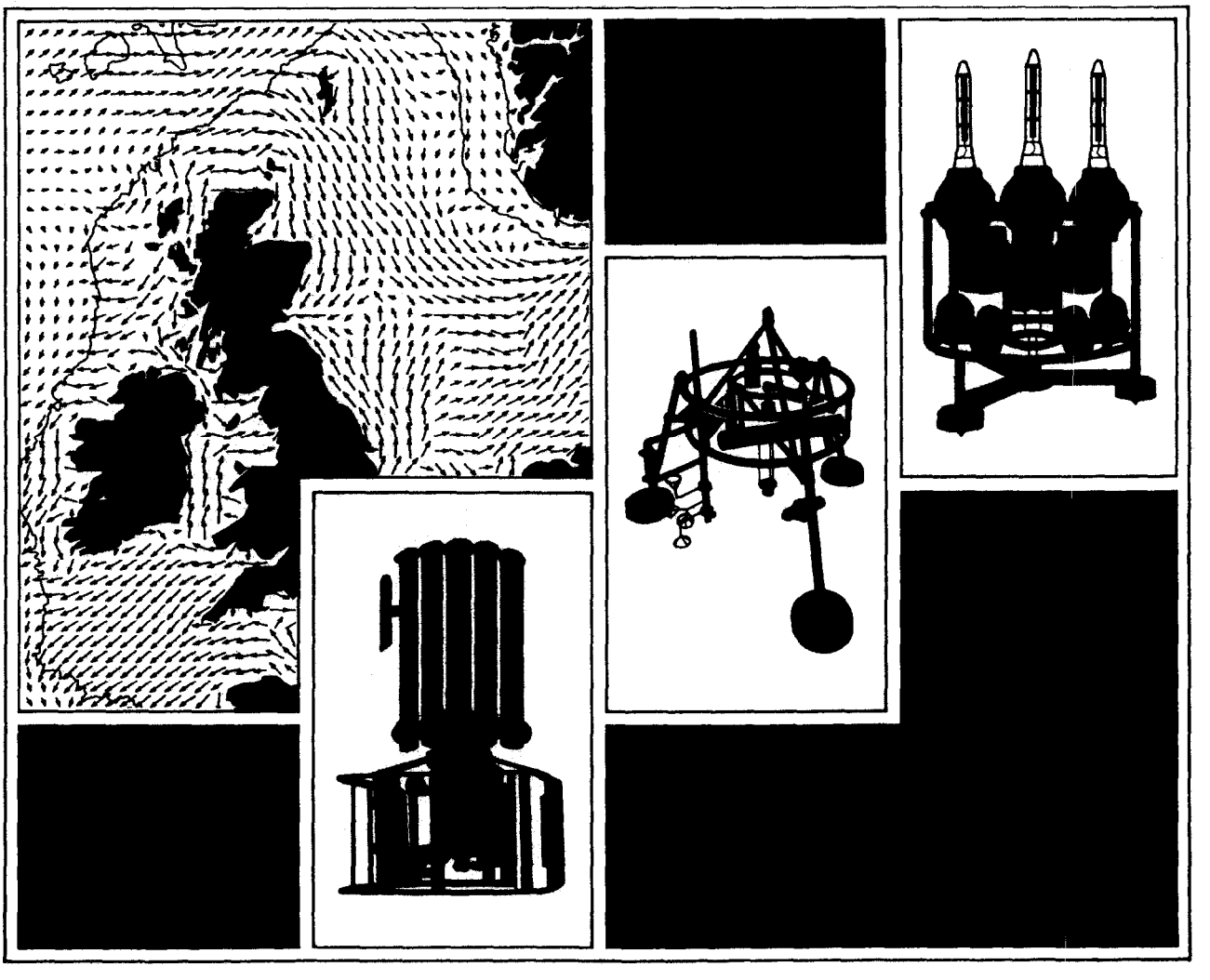

Natural Environment Research Council

PROUDMAN OCEANOGRAPHIC LABORATORY

Bidston Observatory,
Birkenhead, Merseyside, L43 7RA, U.K.

Telephone: 051 653 8633
Telex 628591 OCEANB G
Telefax 051 653 6269

Director: Dr. B.S. McCartney

Natural Environment Research Council

PROUDMAN OCEANOGRAPHIC LABORATORY
REPORT No. 36

MEASUREMENTS OF TURBULENCE AND ACOUSTIC DETECTION OF BEDLOAD IN A MOUNTAIN RIVER

JON J WILLIAMS

1994

DOCUMENT DATA SHEET

AUTHOR
WILLIAMS J J

PUBLICATION DATE 1994

TITLE
Measurements of Turbulence and Acoustic Detection of Bedload in a Mountain River.

REFERENCE
Proudman Oceanographic Laboratory Report Number 36, 40pp.

ABSTRACT

Hydrodynamic measurements obtained using electromagnetic current meters have been used to estimate bed shear stress, apparent bed roughness and the turbulence characteristics of a mountain torrent in Montana, USA. In addition, a sensitive hydrophone has been used to assess the feasibility of deploying an acoustic monitoring system to detect the bedload transport of coarse sediments in remote catchments and to extend the range of existing bedload transport data for model validation purposes. Using appropriate filters, tests show that bedload is detectable above the ambient flow noise.

Acknowledgements
This work was undertaken as part of the MAST II "CSTAB - Circulation and Sediment Transport Around Banks" project. It was funded by NERC and by the Commission of the European Communities Directorate General for Science and Education, Research and Development under contract No., MAS2-CT92-0024. Thanks are extended to Steve Moores and Peter Hardcastle at POL for their help in preparing equipment and to Dr Paul Carling, Harriet Orr and Mark Glaister from IFE for their help during the field work in June 1992.

ISSUING ORGANISATION
Proudman Oceanographic Laboratory
Bidston Observatory
Birkenhead, Merseyside L43 7RA
UK

Director: Dr B S McCartney

TELEPHONE 051 653 8633
TELEX 628591 OCEAN BG
TELEFAX 051 653 6269

KEYWORDS
MONTANA, USA
TURBULENCE
SEDIMENT GENERATED NOISE
BEDLOAD TRANSPORT

CONTRACT
PROJECT MHT-91-5
PRICE £13

Copies of this report are available from:
The Library, Proudman Oceanographic Laboratory.

CONTENTS

1.0 INTRODUCTION

The transport of coarse sediments as bedload and the pursuit of new methods to predict numerically spatial and temporal transport is a subject of considerable interest to oceanographers, hydrologists and engineers. Wide disparities between predictions of bedload transport given by existing transport formulae (Williams et al., 1989a) however, emphasize the need for improved understanding of bedload sediment dynamics to allow development of suitable modelling strategies.

The measurement of both marine and fluvial bedload transport of coarse sediments (grain diameter greater than 5 mm) presents many difficulties in the field and progress in understanding physical processes has been limited by data quality. Difficulties in acquiring suitable field data have arisen owing to problems associated with obtaining simultaneous high temporal resolution measurements of flow and sediment transport during infrequent bedload transport events. Even for moderate rates of bedload transport, relatively high magnitude flows are required to mobilize coarse bed material. Such conditions present a relatively hostile environment for most conventional instrumentation and under flood conditions in a river or large waves in the sea in particular, the destruction of equipment and the consequent loss of data during the most significant transport events is likely. Given further limitations imposed upon field work by the relatively low occurrence frequency of large bedload transport events, it is desirable to deploy robust instrumentation capable of operation under the most extreme conditions and to record observations routinely over a long time period.

The idea of utilizing the noise generated by bedload to quantify coarse sediment transport (sediment generated noise - SGN) with minimal interference with the process appears to have originated with Mühlhoffer (1933). Previous attempts to apply SGN to monitor bedload transport by Bradeau (1951), Juniet (1952), Bedeus & Ivices (1963), Johnson & Muir (1969), Hollingshead (1969, 1971), Samide (1971), Tywonivk & Warnock (1973), Jonys (1976) have met with only limited success. Measurements of bedload in a mountain torrent reported by Bänziger & Burch (1990) have

been obtained using a hydrophone buried beneath a plate in the bed of a stream. During the experiments, the acoustic signature of overpassing particles were not found to correlate with hydrodynamic conditions. Recently however, improved understanding of marine bedload transport processes has resulted from concurrent measurements of flow turbulence and SGN using electromagnetic current meters (ECM's) and a hydrophone respectively, (Heathershaw & Thorne, 1985; Thorne, 1986a). Using a combined theoretical and experimental approach, Thorne (1986b) showed the SGN spectrum to be composed of band-limited noise, with a frequency range inversely proportional to particle size, and an acoustic intensity proportional to the mass of mobile material. The origins of SGN have subsequently been explained theoretically through application of rigid body acoustic radiation theory (Thorne, 1987).

SGN data obtained in the West Solent UK, demonstrate that quasi-fluid bursting events analogous to sweeps (Kline et al., 1967) are correlated strongly with intermittent bedload transport events, (Heathershaw & Thorne, 1985; Thorne, Williams & Heathershaw, 1989; Williams, Thorne & Heathershaw, 1989b) and through careful calibration of SGN data, improved description of mobilization threshold and transport rates has resulted. More recently, attempts have been made to monitor mobilization and transport of gravel under combined wave and current conditions, (Hardisty; Collins *personal communications*). Simulation of bedload transport at time scales commensurate with acoustic measurements reported by Williams & Tawn (1991) utilize statistical techniques. Accurate estimation of instantaneous bedload transport is possible using this approach and through integration allows estimation of total bedload transport. However, the statistical model used presently is site specific and further bedload data for sediments with contrasting grain size distributions in a range of hydrodynamic conditions are required to develop a universal bedload model. The need to acquire new data to extend this work provided the primary motivation for the work reported below.

In the series of field experiments reported here, designed to test instrumentation in exacting conditions and to quantify flow turbulence

and bedload transport, an ECM system modified for the present study and a sensitive hydrophone were deployed in a stream during June 1992 to measure flow turbulence and SGN respectively. Unfortunately, during the time spent in the field, stream stage remained low and little natural bedload transport occurred. However, detailed measurements of the turbulent flow characteristics of the stream were obtained and through artificial production of SGN, it can be demonstrated that acoustic detection of bedload in mountain torrents is now possible with existing equipment.

2.0 FIELD SITE AND INSTRUMENTATION

As a tributary of the Galatin river located near Bozeman, Montana, USA, the field site at Squaw Creek typifies many fast flowing mountain streams in the Rockies and elsewhere (Figure 1). In most years, during the spring, snow melt and frequent convective storms in the upper catchment contribute to rapid diurnal changes in stream discharge. In many instances flows are sufficient to mobilize the coarse bed material and significant bedload transport results. Further details of the field site and of other hydrodynamic and bedload measurements are given by Carling et al. (1994). Given the success in utilizing SGN and ECM turbulence measurements in past marine studies of bedload transport, the present study attempts to apply similar techniques in the energetic environment of Squaw Creek. Whilst being used widely in marine studies of tidal currents and wave hydrodynamics, (eg. Soulsby & Humphery, 1989; Williams et al., 1993), deployment of such instrumentation in shallow, fast flowing rivers has not been attempted before.

The turbulence measuring system employed in the present study was supplied by VALEPORT Instruments, Dartmouth, UK, and consisted of a pair of 10 cm annular open head ECM's and associated electronics. Using a "Y" shape mounting spar, the coil axis of each ECM head was fixed at 45° to the principal flow streamline and at 90° relative to the other (Figure 2). Prior to the fieldwork at Squaw Creek, ECM's were calibrated in a large recirculating flume in the Mechanical Engineering Department at Liverpool University UK. In all cases, ECM sensitivity was approximately

the same (i.e. 0.75 Volt/m/s), the relationship between ECM output and flow velocity was linear and the standard deviation of the current meter measurements at a given velocity was very low (Figure 3).

Measurements of orthogonal turbulent flow components were made using the ECM system positioned at height z = 24 cm above the bed. A sensitive hydrophone was attached close to the current meter heads on the ECM spar at approximately z = 23 cm above the bed (Figure 2). Scour beneath the sensor was not detected in any experiments. Following laboratory tests, unwanted ECM "noise" was reduced by passing output signals through a 15 Hz low-pass filter. A smoothing envelope placed around the output from a log amplifier effectively increases the signal to noise ratio of the hydrophone without compromising the sensitivity to SGN.

Data from the five output channels were sampled at 30 Hz using a data logging system and software developed at POL and were recorded on a laptop PC. Following each measurement campaign, raw data were screened for unwanted noise spikes. In all cases, data quality was high and little editing was required. Figure 4 illustrates schematically the instrumentation and data acquisition system used during the Squaw Creek study.

3.0 MEASUREMENTS AND DATA ACQUISITION

Measurements of flow turbulence and SGN were conducted principally during the period 4 - 8 June, 1992. With stage remaining low, it was necessary to deepen artificially the stream channel and to divert all available flow through the modified section. Following an adjustment period of several hours, when the bed appeared to re-armour, natural flow conditions were re-established and measurements could proceed in a flow depth of approximately 150 cm.

Using a purpose built mounting bracket securely attached to the large timbers of the bridge spanning the upstream portion of the test site (see above), it was possible to position the ECM and hydrophone system at a fixed and stable position above the irregular stream bed, (Figure

2). Despite efforts to ensure the system was rigid, vibration was noted on the ECM mounting spar due to sensor and support oscillation in the fast flow. Possible leakage of this motion into the ECM signals is discussed in 5.1 below.

In general, measurements were obtained over 30 minutes. In other runs, data were recorded over periods of approximately 1.5 hours in order to assess any low frequency modulation of flow and SGN. As flow velocities remained below threshold throughout all the measurements, attempts were made to seed the stream with mobile material by introducing gravel upstream of the sensors. It was considered that such material would be swept downstream beneath the sensors before finding secure resting places. In other instances, particles of different sizes were knocked together manually at approximately 0.5 m from the hydrophone to produce a semi-regular SGN signal with acoustic characteristics not dissimilar to those arising during natural transport of bed material.

4.0 DATA ANALYSIS

4.1 *Introduction*

In this section the methodology used to analyze ECM data are detailed and problems likely to affect data quality and interpretation are highlighted. In general, data processing aimed to quantify flow turbulence, Reynolds stresses and other hydrodynamic characteristics of Squaw Creek. With little bedload transport occurring naturally during the experiments, calibration of the SGN signal using data from magnetic detector logs and bedload traps (Carling et al, 1994) has not been attempted.

4.2 *Data Screening*

All data from the logging system were downloaded via a PC to a workstation. Single files containing ECM and SGN data were prepared for each measurement run and channel numbers assigned to each data set. Raw, uncalibrated data were then plotted and the mean and standard deviation

for each data channel were calculated. These statistics were used as indicators of data quality before proceeding with further analysis.

4.3 *Data Editing*

In order to screen and edit data sets, files were processed using interactive software. This procedure involves the identification of infrequent data spikes by eye and subsequent "flagging" of all suspect points in a given time series. These flags were easily picked up in later processing and were removed using linear interpolations between adjacent good data points. Use of this software also facilitated first look inter-comparisons between data channels and a 'zoom in', 'zoom out' and scan option enabled rapid assessment of data quality.

4.4 *Zero Offsets and Trend Removal*

Zero offset errors were present on all channels. These were measured carefully in the field before and after individual test runs using a large vessel of still water. Following de-spiking, the resulting flume calibrations and offsets were applied to the appropriate data channels in each burst record. A common problem with output from all ECM systems is a tendency for the zero level to drift through time. However, in the case of data described here, the zero drift was very low and linear during test runs and was removed effectively using a least squares trend removal technique.

4.5 ECM *Data Processing*

When deployed, great care was taken to ensure the ECM axis was in line with the principal streamline of Squaw Creek. However, as the accuracy of this technique is subjective, it was necessary to calculate ECM head rotation angles for perfect alignment with the flow. This was achieved by plotting the apparent vertical mean velocity versus the mean horizontal velocity for successive blocks in a given record. Plots of block average vertical (W) versus block average horizontal (U) ECM data for both port (subscript 'p') and starboard (subscript 's') heads show a

general trend corresponding to the mean tilt angle during the experiment. Thus:

vertical rotation angle	$\theta_1 = \tan^{-1}(W_p/U_p)$	;
" " "	$\theta_2 = \tan^{-1}(W_s/U_s)$	;
applying vertical rotation	$W_p = W_p\cos\theta_1 - U_p\sin\theta_1$	;
" " "	$U_p = W_p\sin\theta_1 + U_p\cos\theta_1$	;
" " "	$W_s = W_s\cos\theta_2 - W_s\sin\theta_2$	; and
" " "	$U_s = W_s\sin\theta_2 + U_s\cos\theta_2$	.

In all cases correlation coefficients for the regression W versus U were greater than 95% significant. Uncertainties in zero drift removal, variations in sensor attitude relative to the flow and bed through time and calibration errors combine to give rise to the scatter of data values in such plots.

Following the vertical rotation procedure, a horizontal rotation through 45° (Φ) was then applied to obtain U *(horizontal streamwise)* and V *(horizontal cross-stream)* flow components. This procedure gives time series of the turbulent flow components aligned along the fore/aft and transverse axes of the current meters. Thus:

applying horizontal rotation	$U = (U_a \sin\Phi) + (U_b \cos\Phi)$	; and
" " "	$V = (U_a \cos\Phi) - (U_b \sin\Phi)$	.

Following rotation, software analyzing ECM data produced useful summary statistics (see examples in Table 1). In addition, the following 30 Hz time series were calculated:

current speed	$S = (U^2+V^2)^{1/2}$	;
current direction	$\Psi_c = \tan^{-1}(V/U)$, degrees anti-clockwise of the fore/aft axis	;
fore/aft Reynolds stresses	$Re_1 = \overline{-uw}$, positive downstream	;
transverse Reynolds stresses	$Re_2 = \overline{-vw}$, positive from port to	

starboard ;

stress direction $\Psi_s = \tan^{-1}((\overline{-vw})/(\overline{-uw}))$; and

stress direction re. current $\phi_s = \Psi_s - \Psi_c$.

Estimates of stress magnitude were obtain using the Reynolds stress (or eddy correlation) method (RS) and turbulent kinetic energy method (TKE). Hence:

stress magnitude (RS) $\tau/\rho = ((\overline{-uw})^2+(\overline{-vw})^2)^{1/2}$;

stress magnitude (TKE) $\tau/\rho = 0.19\ \rho\ E$; and

TKE $E = 1/2(\bar{u}^2+\bar{v}^2+\bar{w}^2)$.

4.6 *Errors*

Whilst every precaution was made to exclude errors from the processed data some unwanted "noise" must be tolerated. Error in ECM rotation angle give rise to large error in Reynolds stress values. Using the criteria outlined by Soulsby (1980), it was considered that although suffering from the same minor imperfections, the processed data were acceptably accurate and given further limitations imposed by the physical size of the ECM heads were considered to be representative of turbulent flow conditions in Squaw creek.

5.0 RESULTS AND DISCUSSION

5.1 *Turbulence*

In Figure 5 for clarity, time series plots for the first 0.55 minutes of run 4 show speed, zero-mean turbulent flow components (u, v and w), Reynolds stresses (uw and vw), stress magnitude (τ/ρ), stress direction (Ψ_s) and SGN. In addition power spectra and cospectra obtained for u,v, w, uw and vw are also shown. These energy spectra were obtained from 9.1 minute runs (16384 data values) using a fast Fourier transform (FFT) routine. The raw spectral estimates were smoothed using a weighted averaging scheme and plotted against frequency on log axes (a form generally used for turbulence spectra). The cospectra uw and vw were

obtained by combining raw spectral estimates and subsequently smoothed using a weighted scheme. Cospectra were plotted in the conventional "equal area - equal energy form".

As expected, the statistical distribution of instantaneous u, v and w values were found to be gaussian (Figure 6). In contrast, stress magnitude and SGN series were found to be positively skewed and were characterized by a long tailed distribution (Figures 7a and 7b). Although not demonstrated here, previous studies indicated that the high stress values associated with infrequent "events" shown in Figure 7a were likely to be positively correlated with sediment mobilization, (Williams et al., 1989b). Further discussion and statistical analysis of these distributions is given by Williams & Tawn, (1991). The high frequency, low magnitude SGN events illustrated in Figure 7b were considered to be associated primarily with flow "noise" rather than with sediment transport. In contrast, high magnitude, low frequency events were considered to originate through grain impacts or other acoustic sources at distances away from the hydrophone and showed little correlation with local hydrodynamic conditions (Figure 5). Further consideration of these observations is given below.

The standard deviation for individual 10 minute blocks of ECM data from a continuous measurement period of 1.5 hours showed no significant variation (less than 1 cm/s) through time. Further, spectra obtained for a 1.5 hour record did not exhibit low frequency energy peaks (5-10 minutes) as noted in other geophysical flows, (eg. Lapointe, 1992; 1993). In general, as the typical turbulent eddy sizes scale with flow depth (see below), fluid motions with a period of this order probably originate through a mechanism unassociated with normal production and dissipation processes for turbulent eddies. Whilst not yet confirmed, it has been suggested by Lapointe and others that low frequency turbulent motions in marine, estuarine and large mature river situations may be associated in some way with bedform interactions with flow during active sediment transport. Although differing in flow Reynolds number by a factor of approximately 10 from a shallow marine situation (z = 20 m; S = 1 m/s), and with turbulent eddies scaling more appropriately with flow

depth than with grain size (see below), failure to detect these motions in Squaw Creek, where sediment transportation was negligible and recognizable bedforms were absent, would appear to support this suggestion.

In common with u, v and w time series, instantaneous velocity changes recorded by the ECM system were found to be gaussian and indicated that particles on the bed were likely to be subjected to rapid, high magnitude flow accelerations and decelerations through time (Figure 8). Defining the period of an "event" as being the time during which the velocity of a given flow component continues to rise or fall, Figure 9 shows that short duration events (less than 2.5 seconds) give rise to the the largest acceleration/deceleration terms and exhibit an approximately exponential decay with event length.

As time series obtained in this study correspond more closely to spatial than temporal variations in velocity (Williams et al., 1989b), power spectra obtained using an FFT were converted to wavenumber spectra (not illustrated) by the transform

$$E(k_w) = \{\bar{S}(z)/2\pi\}S(f) \qquad (1)$$

where $E(k_w)$ is the wavenumber spectrum, $k_w = 2\pi f/U(z)$, z is the sensor height above the bed and S(f) is the power spectrum at frequency f. Since frequency is the reciprocal of period (T), the resulting spectra plotted in a normalized form can be used to estimate typical eddy length scale L by

$$k_w = 2\pi \; / \; \bar{S} \; T = 2\pi/L \qquad (2)$$

Thus

$$L = 2\pi z/k_w \qquad (3)$$

At peak spectral values, typical turbulent eddy length scales for u, v and w were found to be approximately 0.52, 0.54 and 0.11 m respectively. Similar results were also obtained through autocorrelation analysis of the time series, (not illustrated here), and indicate clearly that

typical eddies scale with flow depth in Squaw Creek.

Spectra plotted in Figure 5 exhibit a spectral slope values ranging between -1.85 and -2.58 and deviate from the expected value of -5/3. These results demonstrate that fully isotropic conditions do not occur at the maximum spectral wavenumbers in this study. These discrepancies were considered to arise owing to the physical size of the ECM heads and to sampling interval whereby the small scale turbulent motions responsible for energy dissipation were not recorded. This is a common problem with all current measurement devices employed in field studies of turbulence and can lead to underestimation of shear stresses when employing TKE and RS methods (Soulsby, 1980).

Evident on all spectra obtained in Squaw Creek were small peaks at frequency values of approximately 5 Hz. As these were absent in calibration spectra their presence may be attributable to the combined effect of ECM head vibration in the relatively fast flow in Squaw Creek and to regular eddy shedding phenomenon upstream of the test section. Although subject to rapid oscillation in the calibration flume, the narrow frequency band associated with the present spikes however, suggested vibration of ECM's was the primary cause. At worst spectral analysis of the data indicated that the presence of these spurious "turbulence" signals results in an overestimation of bed shear stress of $< 5\%$.

5.2 *Bed Shear Stress and Turbulence Intensity*

It is generally accepted that the "constant stress layer" of a fully developed turbulent boundary layer occupies approximately the first 10% of total boundary layer thickness and measurements of Reynolds stresses within this region yield an approximation to bed shear stress. Given a flow depth at the present study site of approximately 150 cm, Reynolds stress approximations were only likely to be valid therefore for z up to 15 cm. Further, given the nature and arrangement of the coarse particles comprising the bed, this assumption is likely to be misleading owing to the presence of an *internal* boundary layer where turbulence probably

scales with particle size and an *outer layer* with flow scales approximating to the largest roughness elements and the characteristic length scale of the *internal* boundary layer turbulence (Carling et al., 1994). It would not be expected therefore, that present measurements obtained at z = 24 cm would give results that relate to bed shear stresses directly. Derived U_* values from the present ECM system would also be expected to differ from those obtained using a log profile (LP) fit to detailed velocity profile data obtained by Carling et al. (1994) using a small ECM probe (Table 2).

Values of U_* in Table 2 obtained using TKE and RS methods however, were not only very consistent during measurement runs 4 - 8, but were also similar in magnitude to U_* values obtained using the log profile method (Carling et al., 1994). Estimates of U_* obtained using the TKE method were however, consistently lower than those obtained using the RS method. These differences were considered to arise owing errors in ECM head alignment relative to the main streamline and were brought about principally by secondary flows within the channel. In contrast to the TKE method, the RS method has been shown to be especially sensitive to such errors (Hannay et al, 1994). On the basis of these results it would appear that despite the limitations of the present ECM system outlined above, U_* estimates obtained in the highly turbulent flow conditions using data from independent sensors and different analysis techniques give approximately the same results.

When normalized using U_* values obtained using the TKE approximation ($U_* = (\tau/\rho)^{0.5}$, see below), RMS turbulence intensity values for turbulent flow component x (i.e. β_x), defined as $\beta_x = \sigma_x/U_*$, where σ_x is the standard deviation of flow component x, showed a high degree of consistency and ranged between 1.9 - 2.3, 2.2 - 2.3 and 1.0 - 1.6 for u, v and w respectively. These values were in good agreement with those obtained in other geophysical flows (e.g. Soulsby, 1983). Relatively steady flows during the measurement periods prevented study of RMS turbulence levels over a range of flow conditions.

5.3 *Apparent Bed Roughness*

Table 2 shows drag coefficient (Cd) and apparent bed roughness (Z_a) values obtained using the following empirical approximations:

$$Cd(z) = 1/2\ (\{U_* \text{ TKE }\}^2 + \{U_* \text{ RS }\}^2)/\ \bar{U}^2 \qquad (4)$$

where Cd(z) is a drag coefficient at height z = 24 cm, U_* TKE is the shear velocity value derived from turbulent kinetic energy and U_* RS is the shear velocity value derived from Reynolds stresses. The apparent bed roughness is defined as

$$Z_a = z\ e^{(-k/Cd[z]^{0.5})} \qquad (5)$$

where k is von Kármán's constant = 0.4. In common with U_* values, Cd and Z_a values were generally consistent over runs 4 - 8 and were lower than those derived using the log profile method (Carling et al., 1994). Detailed velocity profiles taken through the *constant stress* layer and the *outer-layer* indicated the presence of an inflection above the near-bed layer and lead Carling et al. (1994) to conclude that Squaw Creek was characterized by two scales of roughness: (a) Z_a values obtained from detailed velocity profiles which scale with the grain size of the bed material; and (b) Z_a values obtained from profile segments in the *outer-layer* which probably scale the wake layer adjacent to bed particles.

5.3 SGN *Measurements*

Time series plots of SGN in Figure 5 showed little visual correspondence with any flow parameter obtained using the ECM measurements. This has been confirmed from cross correlation analyses using 30 minute time series. Further, the spectrum of SGN was closely similar to that for u (Figure 10), and for SGN output in flows without sediment transport. This suggests strongly that the hydrophone was only recording flow "noise". Attempts to seed Squaw Creek with copious amounts of mixed grain size particles on a number of experimental runs failed to produce

correlation between SGN and bedload transport (see Figure 10). These results were recognized in the field during preliminary data analysis and thus an alternative experimental technique was sought.

Selected particles from the bed were collected and sorted by size. By gently knocking particles together underwater at a distance of 0.5 m away from the hydrophone it was possible to detect and record the resulting SGN signal for a range of sizes and positions from the sensor. During experimental runs over approximately 1 minute, attempts were made to produce regular collisions between the test particles in order that they may be more clearly identified in the hydrophone record. In the event this proved to be unnecessary as the resulting SGN level was found to be significantly above the background acoustic noise of Squaw Creek.

SGN data typifying an impact test at 1.0 m from the hydrophone using well rounded particles with a diameter in the range 32-64 mm is shown in Figure 11. In common with previous plots, SGN is shown on a logarithmic scale. The near regular peaks present in Figure 11 rise by at least two orders of magnitude above the "background" level and thereby provide convincing evidence that SGN could be detected in Squaw Creek. This is illustrated further in Figure 12 which shows SGN and u spectra on the same axes. Here, in contrast with Figure 10, the spectral characteristics of u and SGN differ significantly over the range of frequencies shown. Given these clear results and the lack of natural bedload transport data, no further analysis of the SGN data was attempted.

6.0 CONCLUSIONS

During the relatively low flow conditions prevailing in Squaw Creek during early June 1992 it has been possible to obtain good quality measurements of flow turbulence. Further, through local generation of SGN it has been shown that acoustic detection of bedload in fast flowing, gravel bed streams is possible using the present detection system.

The following conclusions were reached from the experimental results:

6.1 With appropriate scaling, the statistical properties of u, v and w time series were found to be consistent with measurements obtained in other geophysical flows.

6.2 In common with other natural flows over rough boundaries, the bulk of Reynolds stress production in Squaw Creek was associated with infrequent 'events'. In general 'events' have a duration greater than 1.5 seconds and a return period greater than 10 seconds.

6.3 Typical eddy length scales determined using wavenumber spectra and autocorrelation functions were found to be 0.52, 0.54 and 0.11 m for u, v and w respectively. However, given flow structure limitations imposed by the physical size of the ECM heads these length scales may be subject to error.

6.4 Spectral slope values in the range -1.85 to -2.58 demonstrated that fully isotropic conditions were not detected using the present sensors. This was considered to arise through a combination of circumstances including: selection of record length; digitisation rate; low-pass filter cut-off; and the physical size of the ECM heads. With present data, it was not possible to determine the significance of any single factor identified.

6.5 Owing to ECM head misalignment problems, bed shear stress values obtained from ECM measurements using the TKE methods were found to be consistently lower than those determined using the RS method. Further, location of the ECM sensors well outside the "law of the wall" region, high bed roughness values and factors outlined in 6.4 above probably contributed to the disparity between U_* values obtained using these methods and some of those obtained using the log profile method. In general, however, U_* values obtained here were in good agreement and were thought to be reliable indicators of bed shear stress in Squaw Creek.

6.6 Drag coefficient and roughness length values obtained using the present measurements of bed shear stress and flow speed were found to be consistent and in general agreement with published values for similar sediments. Z_a and Cd values obtained here were considered to be fairly reliable indicators of hydraulic roughness experienced by the outer-layer 'wake' flow in Squaw Creek.

6.7 Owing to the low flow in Squaw Creek, mobilization of bed sediments did not occur. Attempts to seed the flow with mobile material were not detected by the present acoustic sensor.

6.8 Manual generation of SGN at 0.5 m from the hydrophone using a range of selected pebble sizes produced acoustic energy significantly higher than the background in Squaw Creek. SGN generated in this way was easily detected and, based upon past experience, was considered to be typical of SGN arising during natural bedload transport.

Whilst conditions in Squaw Creek during the experimental period in early June were far from ideal, it has been established for the first time that acoustic detection of bedload in a fast flowing mountain torrent is possible. There is the possibility therefore, of utilizing such a system to monitor field sites and to transmit data indicating the mobility status of a given bed sediment directly to a remote receiving station. Such a system would aid river management strategies in inaccessible areas and would provide further useful data to aid understanding of catchment flood response and fluvial sedimentary processes. Further, the present experiments indicate that SGN measurements may also be possible in marine environments (e.g. the surf zone) where ambient acoustic noise is large. In view of these promising results, further experimental investigation of the present measurement system during periods of active bedload transport will be pursued.

7.0 REFERENCES

BÄNZINGER, R. & BURCH, H. 1990 Acoustic sensors (hyrophones) as indicators for bed load transport in a mountain torrent. Hydrology in Mountainous Regions. I - Hydrological Measurements; the Water Cycle. IAHS Publ. No. 193, 207-214.

BEDEUS, K. & IVICSICS, L. 1963 Observations of the noise of bedload. Proceedings of the International Association of Science and Hydrology, Publication Number 65, 87pp.

BRADEAU, G. 1951 Quelques techniques pour l'étude et la mesure du débit solide. La Houille Blanche, Spéc. No. A, 54pp.

BUNTE, K., CUSTER, S. G., ERGENZINGER, P. & SPIEKER, R. 1987 Messung des Grobgeschiebetransportes mit der Magnettracertechnik. Deutsche Gewasserkundliche Mitteilungen, 31, 60-67.

CARLING, P. A., WILLIAMS, J. J., GLAISTER, M. G. & ORR, H. G. 1994 Dynamics of gravel transport and turbulent flow in a mountain river. Water Resources Research (In press).

HANNAY, A., WILLIAMS, J. J., WEST, J. R. & COATES, L. E. 1994 Field measurements of wave:current interactions over a rippled sand bed. Proceedings of Euromech 310, Sediment Transport Mechanics in Coastal Environments and Rivers, (eds. M. Belorgey & J. A. F. Sleath), 13 - 17 September 1993, Le Harvre, France, 10pp.

HEATHERSHAW, A. D. & THORNE, P. D. 1985 Sea-bed noises reveal role of turbulent bursting phenomenon in sediment transport by tidal currents. Nature, 316, 339-342.

HOLLINGSHEAD, A. B. 1969 Sediment transport measurements in Elbow River at Bragg Creek. Report to Cooperative Agencies, Research Council of Alberta, 67pp.

HOLLINGSHEAD, A. B. 1971 Sediment transport measurements in a gravel river. Journal of Hydraulic Research, 97(HY11), ASCE, 235-247.

JOHNSON, P. & MUIR, T. C. 1969 Acoustic detection of sediment movement. Journal of Hydraulic Research, 7(4), 519-540.

JONYS, C. K. 1976 Acoustic Measurement of Sediment Transport. Scientific Series Number 66, Inland Water Directorate, CCIW Branch, Burlington, Ontario, 118pp.

JUNIET, M. 1952 L'Arénaphone, un appareil détecteur des mouvements des sédiments fins. Transport Hydraulique et Decantation des Materiaux Solides, Société hydrotechnique de France, 39pp.

KLINE, S. J., REYNOLDS, W. C., SCHRAUB, F. A. & RUNDSTADLER, P. W. 1967 The structure of turbulent boundary layers. Journal of Fluid Mechanics, 30, 741-73.

LAPOINTE, M. F. 1992 Burst-like sediment suspension events in a sand bed river. Earth Surface Processes and Landforms, 17, 253-270.

LAPOINTE, M. F. 1993 Monitoring allivial sand suspension by eddy correlation. Earth Surface Processes and Landforms, 18, 157-175.

MÜHLHOFFER, L. 1933 Untersuchungen über die Schwebstoff und Geschiebeführung des Inn bei Kirchbichl die Wasserwirtschaft, No. 2, 43pp.

SAMIDE, G. W. 1971 Sediment transport measurement. MSc. Thesis, Univ. Alberta, 167pp.

SOULSBY, R. L. 1980 Selecting record length and digitization rate for near-bed turbulence measurements. Journal of Physical Oceanography, 10, 208-219.

SOULSBY, R. L. 1983 The bottom boundary layer in shelf seas. pp. 189-266 in: Physical Oceanography of Coastal and Shelf Seas, (ed. B. Johns). Amsterdam: Elsevier, 470pp. (Elsevier Oceanography Series, 35)

SOULSBY, R. L. & HUMPHERY, J. D. 1989 Field observations of wave-current interaction at the sea bed. pp 413-428 in Water Wave Kinematics, (Eds. A. Torum & O. T. Gudmestad), Dordrecht: Kluwar Acedemic, 771pp.

THORNE, P. D. 1986a Laboratory and marine measurements on the acoustic detection of sediment transport. Journal of the Acoustics Society of America, 80, 899-910.

THORNE, P. D. 1986b An intercomparison between visual and acoustic detection of seabed gravel movement. Marine Geology, 72, 11-31.

THORNE, P. D. 1987 The acoustic measurement of gravel transport. pp. 63-70 in, Fifth International Conference for Ocean Technology, Heriot-Watt University, Edinburgh, 1987. London: Institution of Electronic and Radio Engineers, 225pp. (IERE Publication Number 72)

THORNE, P. D., WILLIAMS, J. J. & HEATHERSHAW, A. D. 1989 In situ acoustic measurements of marine gravel threshold and transport. Sedimentology, 36, 61-74.

TYWONIUK, N. & WARNOCK, R. G. 1973 Acoustic detection of bed-load transport. Fluvial Processes and Sedimentation, Proceedings of the 9th Canadian Hydrology Symposium, Ottawa, Canada, 728-749.

WILLIAMS, J. J., THORNE, P. D. & HEATHERSHAW, A. D. 1989a Comparisons between acoustic measurements and predictions of the bedload transport of marine gravels. Sedimentology, 36, 973-979.

WILLIAMS, J. J., THORNE, P. D. & HEATHERSHAW, A. D. 1989b Measurements of turbulence in the benthic boundary layer over a gravel bed. Sedimentology, 36, 959-971.

WILLIAMS, J. J. 1990 Video observations of marine gravel transport and threshold. Geo-Marine Letters, 10(3), 157-164.

WILLIAMS, J. J. & TAWN, J. A. 1991 Simulation of bedload transport of marine gravel. pp. 703-716 in, Coastal Sediments '91, (N. C. Kraus, K.J. Gingerich and D. L. Kriebel) Volume 1. New York: American Society of Civil Engineers, 2360pp. (2 volumes.)

WILLIAMS, J. J., HARDCASTLE, P. J. & HUMPHERY, J. D. 1993 Hydrodynamic conditions leading to the resuspension of marine sediments. Continental Shelf Research (in press)

8.0 SYMBOLS, ACRONYMS AND ABBREVIATIONS

E	turbulent kinetic energy (m^2/s^2)
$E(k)$	wavenumber spectrum (m^2/s^2)
g	acceleration due to gravity (m/s^2)
k	von Karmans constant (0.4)
k_w	wavenumber
L	typical eddy length scale (m)
p	(subscript) port
s	(subscript) starboard
S	mean current speed (m/s)
$S(f)$	power spectrum (m^2/s^2)
T	period (s)
U	streamwise flow component (m/s)
U_*	bed shear velocity (m/s)
u'	streamwise current flow component (m/s)
$u_t'^2$	streamwise turbulence variance (m^2/s^2)
V	cross-stream flow component (m/s)
v'	cross-stream current flow component (m/s)
$v_t'^2$	cross-stream turbulence variance (m^2/s^2)
w'	vertical flow component (m/s)
$w_t'^2$	vertical turbulence variance (m^2/s^2)
z	height above the bed (m)
Z_a	apparent bed roughness (m)
θ	ECM vertical rotation angle (degrees)
ρ	fluid density (1027 Kg/m^3)
σ	sediment density (2650 Kg/m^3)
σ	standard deviation
τ	bed shear stress (N/m^2)
ν	kinematic viscosity (m^2/s^2)
ψ_c	current direction (degrees)
ψ_s	stress direction (degrees)
ϕ_s	stress direction relative to current (degrees)

BODC	British Oceanographic Data Centre
ECM	Electromagnetic current meters
FFT	Fast Fourier transform
IFE	Institute of Freshwater Ecology
LP	Logarithmic profile
POL	Proudman Oceanographic Laboratory
RS	Reynolds stress method
SGN	Sediment generated noise
TKE	Turbulent kinetic energy

Summary of Squaw Creek Data Analysis, Run 4, 12h34 P.S.T, 4/6/92.	
Measurement period	= 30 minutes
Logging speed	= 30 Hz
Average current speed	= 133.1 cm/s
σ_u	= 10.6 cm/s
σ_v	= 11.6 cm/s
σ_w	= 6.0 cm/s
U_* TKE	= 5.2 cm/s
U_* RS	= 7.9 cm/s
Cd	= 0.0025
Z_a	= 0.0081 cm

Table 1. Useful data summary statistics output during initial processing of Squaw Creek data.

Parameter	Experiment Number				
	4	5	6	7	8
S, cm/s	133.1	131.0	131.2	125.8	127.6
σ_u cm/s	10.6	11.3	11.1	12.3	10.6
σ_v cm/s	11.6	12.6	12.2	11.9	11.6
σ_w cm/s	6.0	5.7	6.0	5.3	9.0
U_* (TKE) cm/s	5.2	5.6	5.4	5.5	5.6
U_* (RS) cm/s	7.9	7.9	8.1	7.8	9.9
‡ U_* (LP) cm/s	10.5	16.2	6.1	8.6	10.7
Cd x 10^{-3} (Eq.4)	2.5	2.7	2.8	2.9	3.9
Z_a x 10^{-2} cm (Eq.5)	0.8	1.0	1.0	1.3	3.9
‡ Z_a cm (LP)	0.8	2.1	0.1	0.5	0.7

Table 2. Summary of: current speed (S); standard deviation values for u, v and w (σ); U_* ; and Z_a values from TKE, RS and LP measurements, experiments 4 - 8, Squaw Creek, June 1992.(‡ *from Carling et al., 1994*)

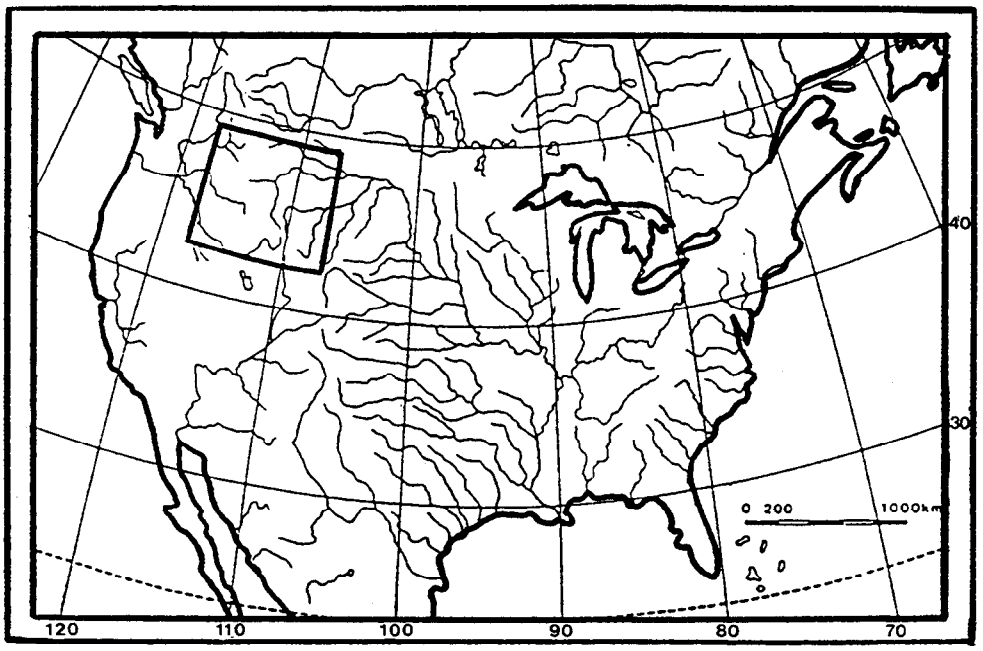

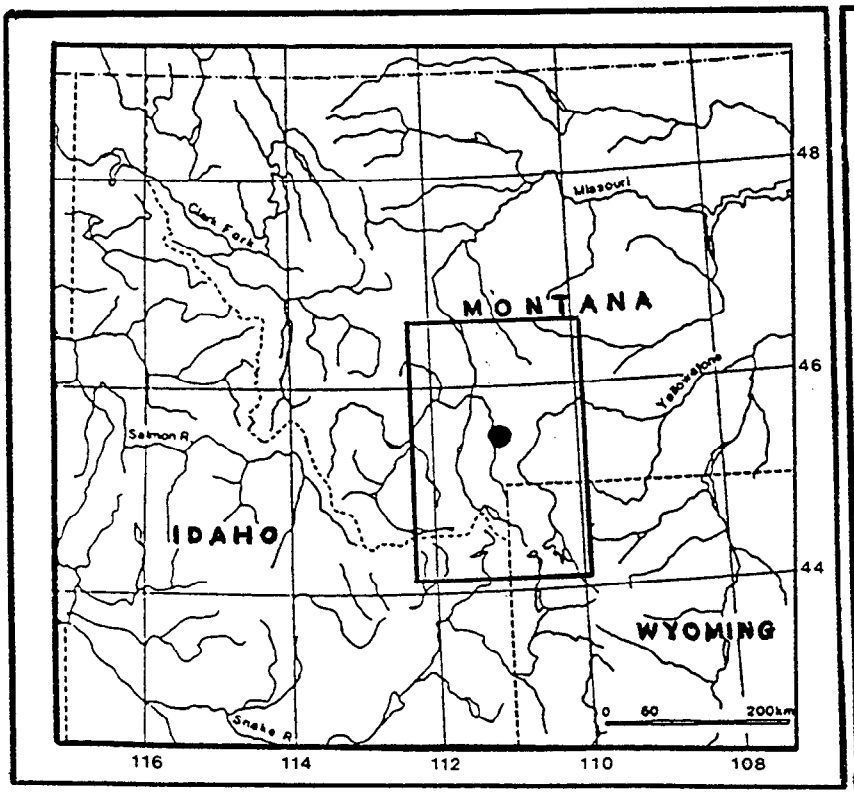

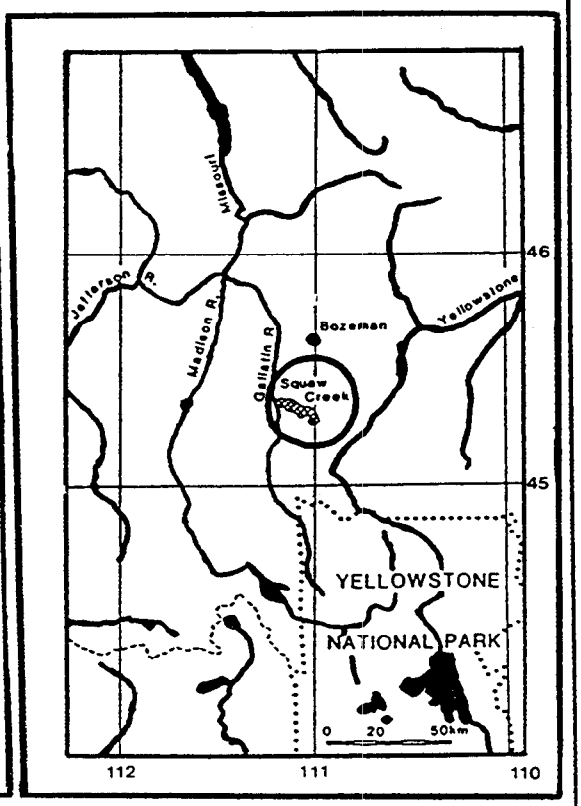

FIGURE	Location of the field site in Montana, USA *(after Bunte et al., 1987).*
1	

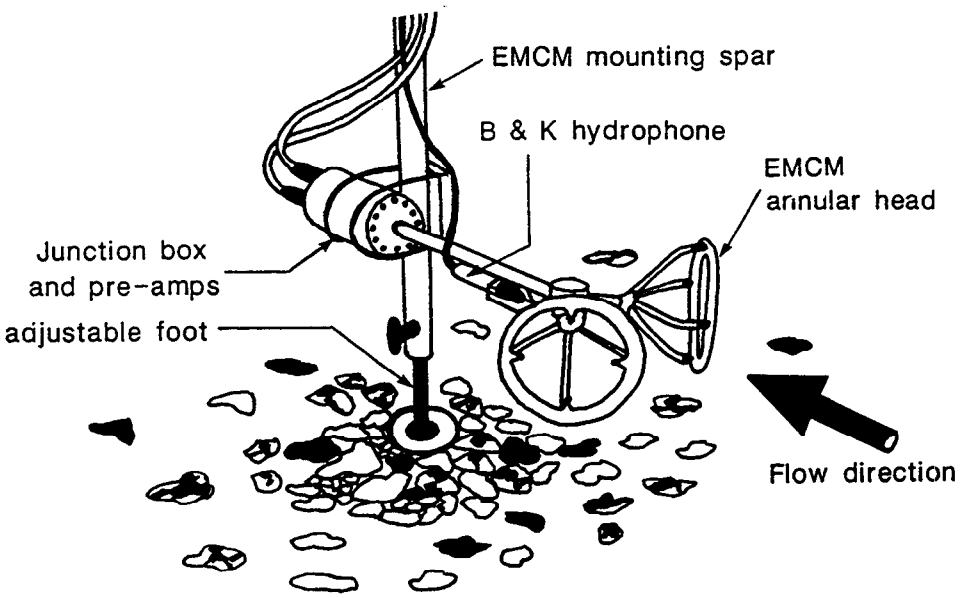

FIGURE	ECM and hydrophone system deployed in Squaw Creek in June 1992.
2	

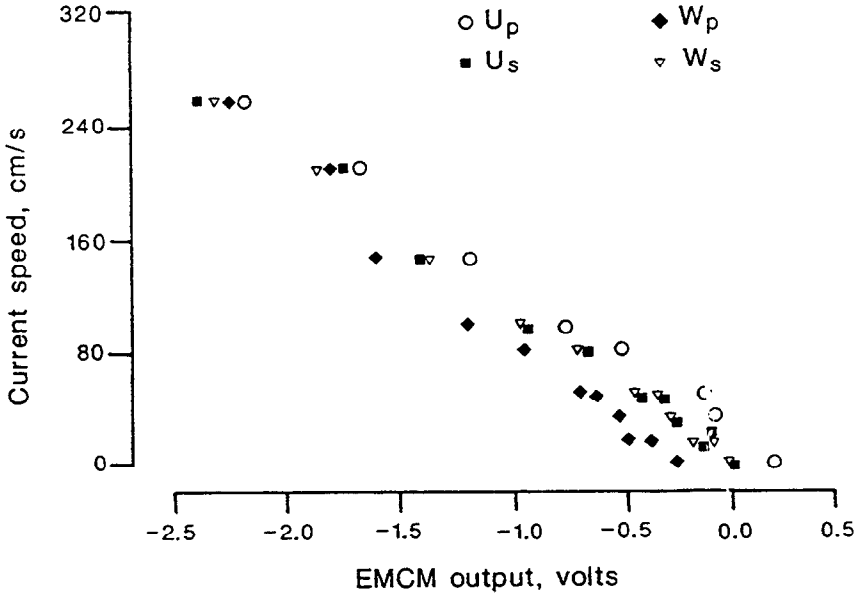

FIGURE	
3	ECM calibration for port (p) and starboard (s) horizontal (u) and vertical (w) channels. In all cases $r^2 > 0.995$.

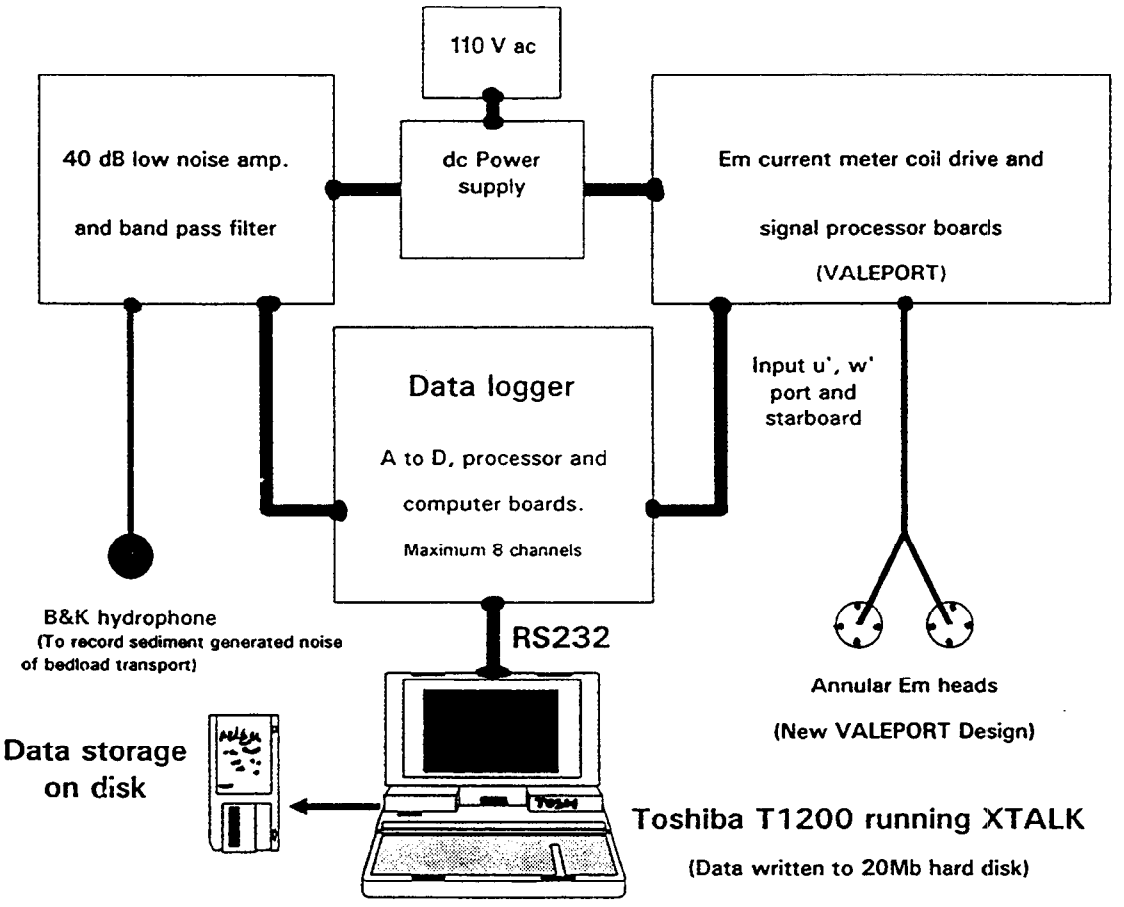

FIGURE	
4	Instrumentation and data acquisition system used in the Squaw Creek study.

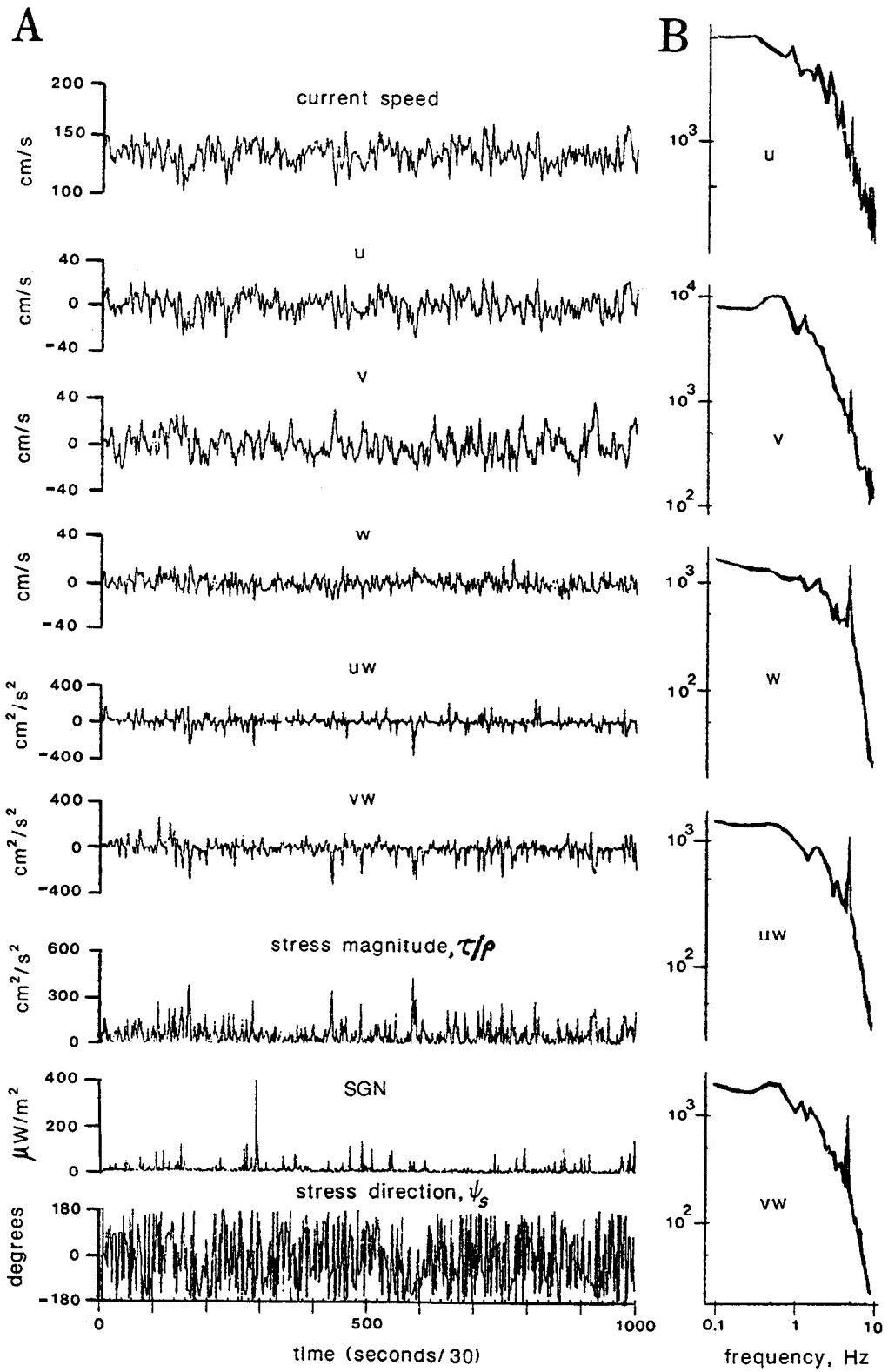

For clarity, only the first 33 seconds of the time series records are illustrated.

FIGURE	(a) Time series plots of S, u, v, w, uw, vw, τ/ρ, SGN and ψ_s; and
5	(b) u, v and w spectra and uw, vw cospectra, run 4, Squaw Creek.

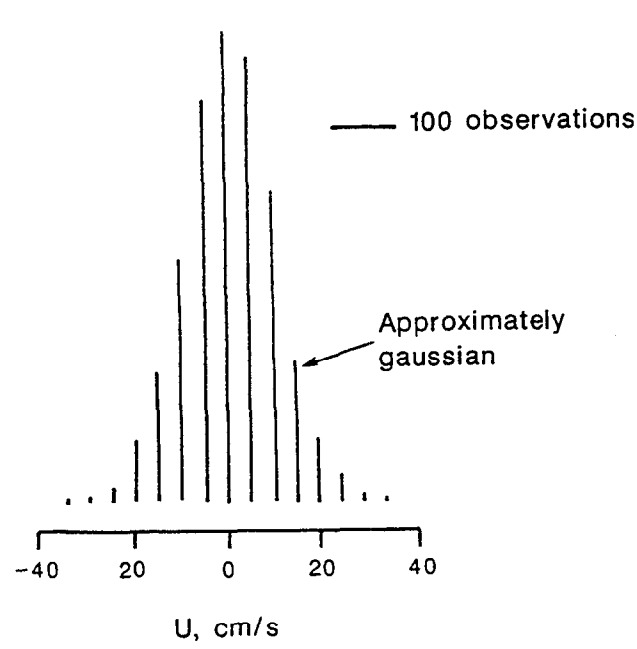

FIGURE 6	Instantaneous streamwise flow component (u), run 5, Squaw Creek.

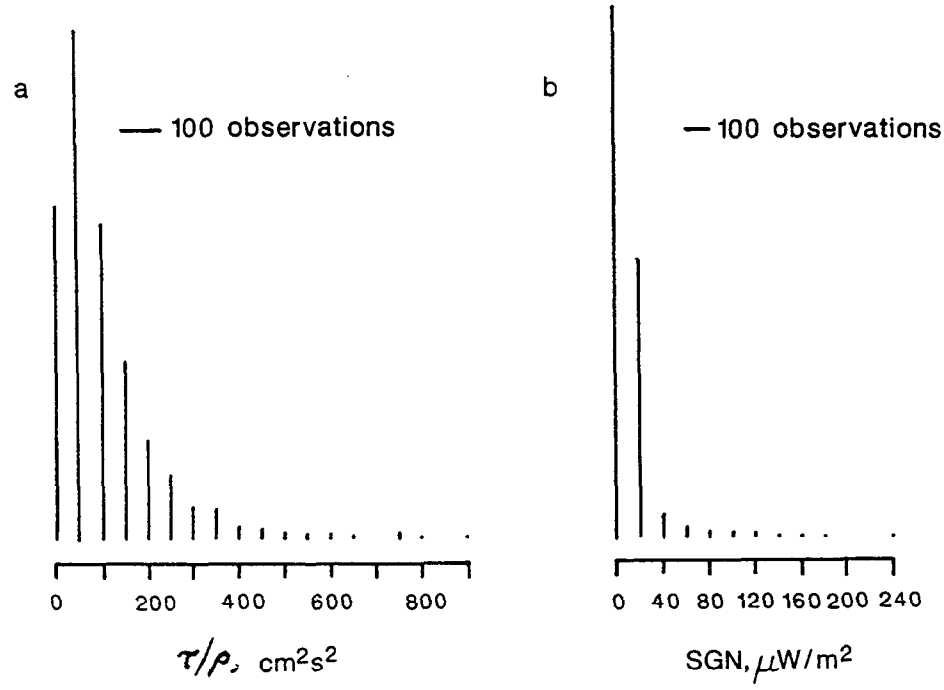

FIGURE 7	Instantaneous (a) stress magnitude (τ/ρ); and (b) SGN.

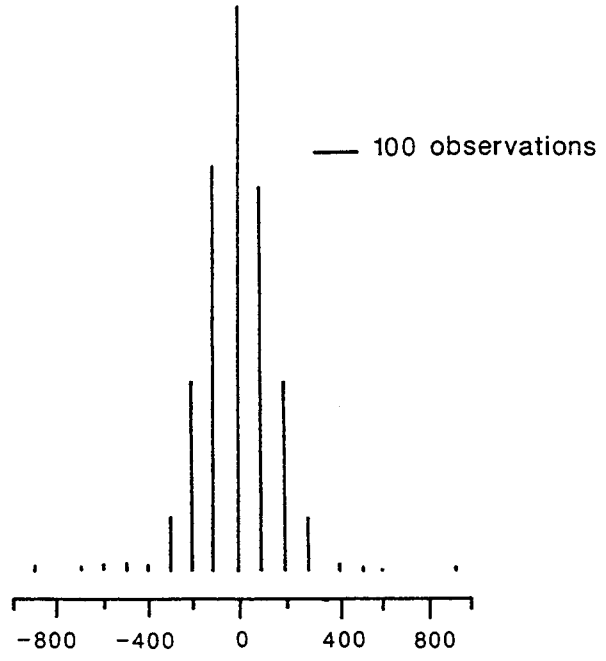

FIGURE 8	Instantaneous acceleration of streamwise flow component (du/dt).

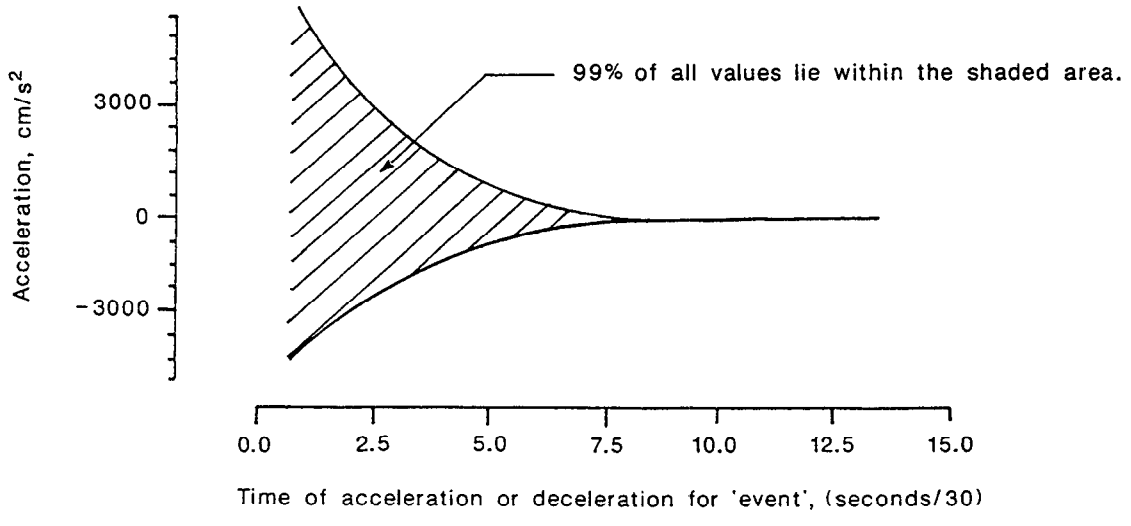

FIGURE 9	Acceleration/deceleration associated with an "event" of given duration.

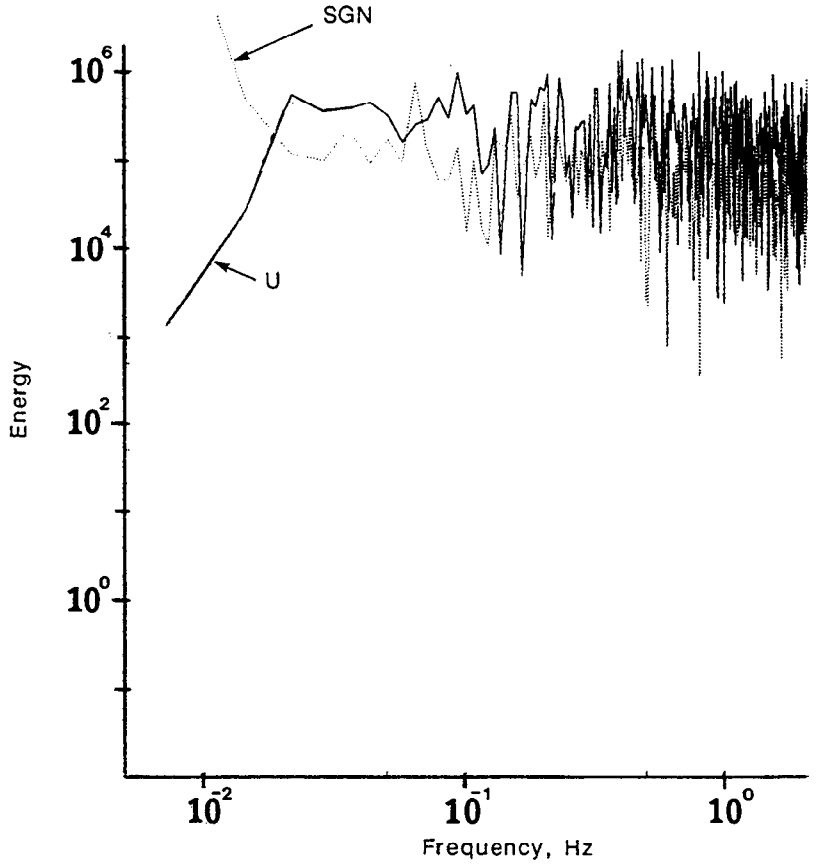

FIGURE	
10	Spectra obtained from streamwise flow component u and SGN during a bedload seeding experiment.

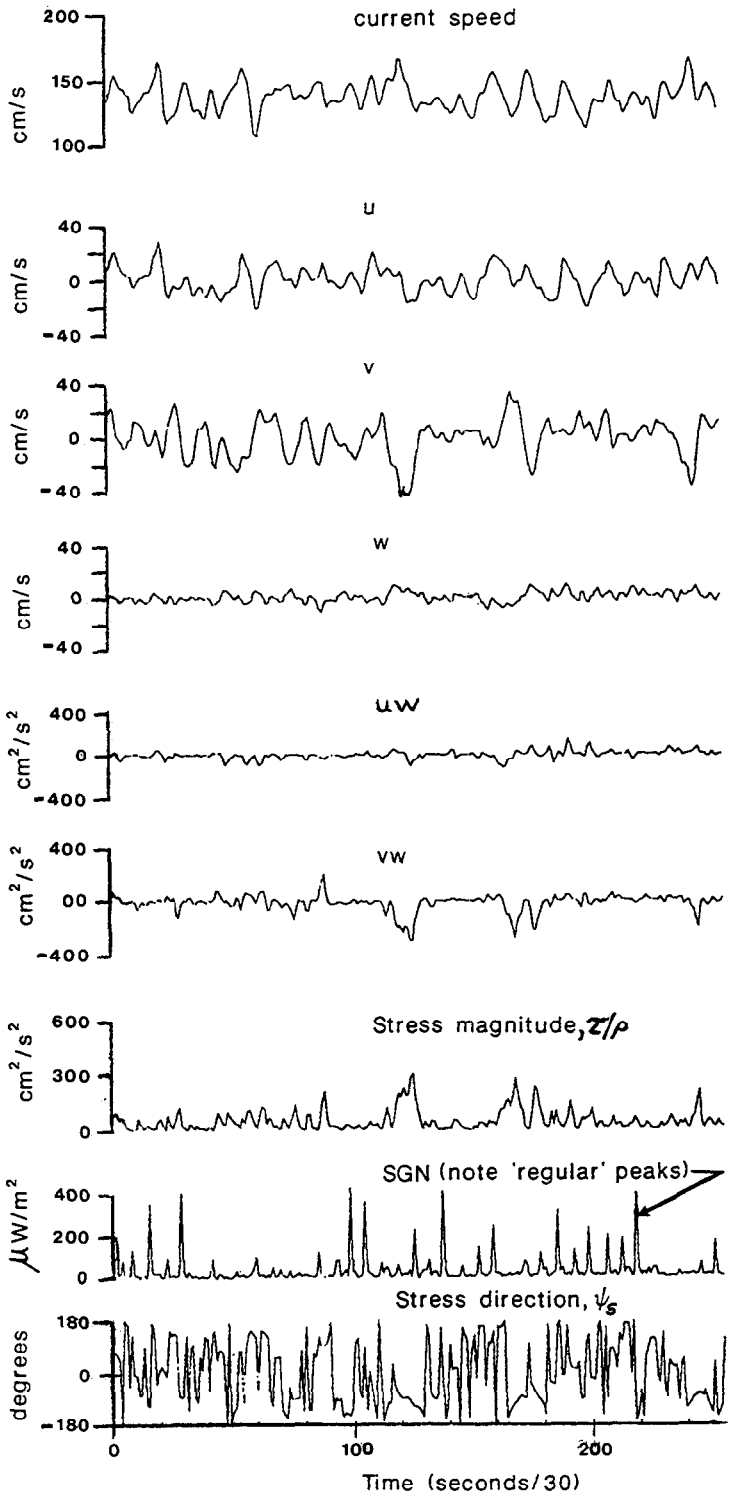

FIGURE	Time series plots of S, u, v, w, uw, vw, τ/ρ, SGN and ψ_s obtained during a typical grain impact test.
11	

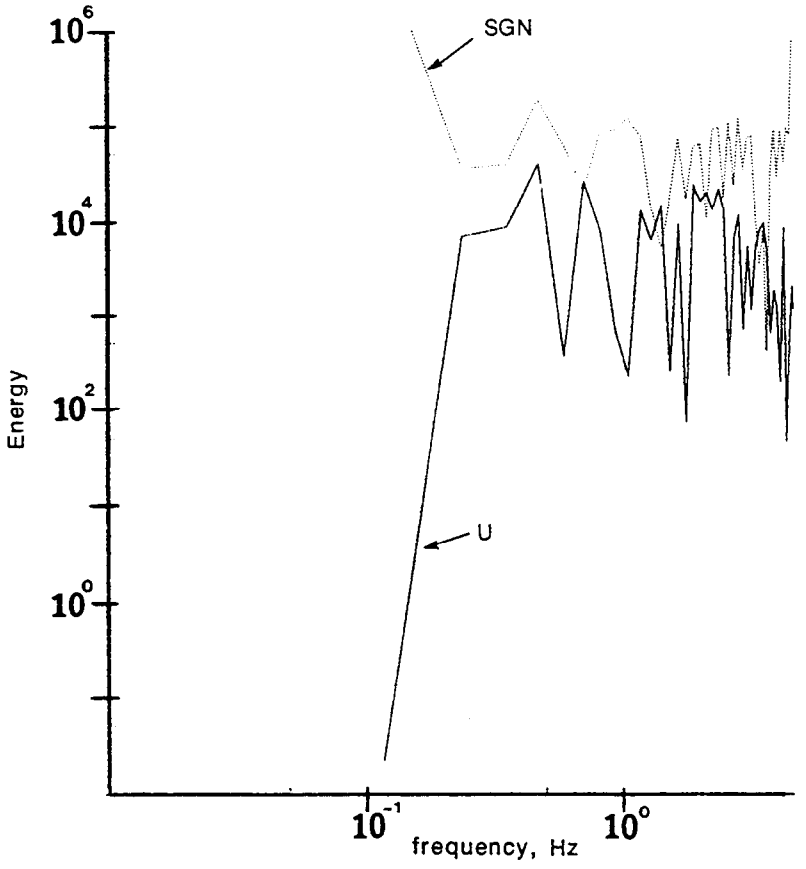

FIGURE	
12	SGN and streamwise flow component (u) spectra derived from measurements obtained during a grain impact test.